RSC Advances

PAPER

View Article Online
View Journal | View Issue

Cite this: RSC Adv., 2015, 5, 84216

High pressure Raman spectroscopy investigation on acetonitrile and acetonitrile–water mixture

Chen Chen, Xiaoli Huang, Dongxiao Lu, Yanping Huang, Bo Han, Qiang Zhou, Fangfei Li* and Tian Cui

Received 12th July 2015
Accepted 30th September 2015

DOI: 10.1039/c5ra13639c

www.rsc.org/advances

High-pressure Raman scattering studies on pure acetonitrile and an acetonitrile–water mixture at a molar ratio of ($n$$CH_3CN$: $n$$H_2O$) 1 : 7.25 were performed in a diamond anvil cell at room temperature. The structural transitions of pure acetonitrile from liquid to α phase, α to β phase and β to γ phase were detected from Raman spectra variations at 0.2 GPa, 0.8 GPa and 4.95 GPa, respectively. The acetonitrile–water mixture presented a much higher solidification pressure of 1.25 GPa and the β phase is found to be sustained up to 7 GPa. Through Raman analysis on the solid acetonitrile–water mixture, the acetonitrile clusters were found to exist as separated domains and surrounded by ice crystal domains due to large amounts of water in the mixture. Meanwhile the fluorescence was obviously depressed in the mixture and the Raman peaks can be detected up to 29.88 GPa, while the Raman peaks in pure acetonitrile are undetectable at 21 GPa due to its increased fluorescence.

Introduction

Acetonitrile (CH_3CN) is one of the most stable nitrile compounds with excellent solvent properties; it turns out to be a typical molecular crystal at low temperature or under high pressures, which has been previously studied by spectroscopic and X-ray diffraction studies.[1–6] Acetonitrile is miscible with water or alcohol in any proportion at ambient pressure and room temperature. The mixtures of acetonitrile and water are extensively used in many fields such as organic synthesis, chromatography, electrochemistry and solvent extraction, due to its peculiar properties different from other traditional organic solvents.[7–9] For example, the highly charged ion pair complexes can be extracted only by acetonitrile–water mixtures instead of other conventional organic solvents such as chloroform.[10,11]

As a kind of binary solution, acetonitrile–water mixtures have very complicated interactions in the system, many studies have been performed on acetonitrile–water mixtures by various methods, including infrared spectroscopy (IR),[12–14] X-ray diffraction (XRD),[15,16] thermodynamic,[17–21] Raman spectroscopy,[22–24] theoretical simulations[25–27] and unclear magnetic resonance spectroscopy (NMR).[28–30] Previously, Takamuku *et al.* have investigated the liquid structure of acetonitrile–water mixtures by XRD study.[15] They found that in pure acetonitrile, one acetonitrile molecule interacts with two neighbouring molecules through an antiparallel dipole–dipole interaction combined with a small shift of their molecular center resulting in a zigzag cluster. After mixed with water, the hydrogen bond is expected to participate in and the structure of the mixture can be divided into three regimes depending on concentration distribution.[31] For the water rich mixture ($X_{AN} \leq 0.2$, where X_{AN} means the mole content of acetonitrile), small acetonitrile clusters are isolated from extended water hydrogen bond network, and for the acetonitrile rich mixture ($X_{AN} \geq 0.8$), the water molecules would be surrounded by extended acetonitrile network forming small water clusters or staying isolated. If X_{AN} is between 0.2 and 0.8, it is suggested to be coexistence of large clusters of water and acetonitrile molecules. In this region it is pointed out that the microheterogeneity which is a common feature in the mixed solvent also exists in acetonitrile and water solution, *i.e.* molecules are preferably surrounded by the same kind of component and leads to the formation of small aggregates consisting entirely of one type molecules, then the system exhibit spatial inhomogeneities at the microscopic scale but is homogeneous macroscopically.[12,15,18,32]

Previous investigations are mainly focused on the structural changes in liquid mixture and discussion on the effect of the content ratio variation at room pressure and temperature or low temperature. However, the pressure induced variation of acetonitrile water mixture is still unknown. We know that if the system in the neighbourhood of the critical point, there should be giant fluctuations of density and concentration in the mixture,[33–35] resulting in structural and properties changes. Increasing pressure also plays a similar role of lowing temperature. So in this work, we performed *in situ* high-pressure Raman scattering measurements on both pure acetonitrile and acetonitrile–water mixture with a molar ratio of ($n$$CH_3CN$: $n$$H_2O$) 1 : 7.25 in a diamond anvil cell (DAC).

State Key Laboratory of Superhard Materials, College of Physics, Jilin University, China. E-mail: lifangfei@jlu.edu.cn

Pressure induced vibrational and structural transitions in two systems are obtained and compared.

Experimental

Acetonitrile was purchased from Alfa Aesar (>99.8%) without further purification. Pure acetonitrile and distilled de-ionized water were mixed in molar ratio of 1 : 7.25 ($n$$CH_3CN$: $n$$H_2O$) for this study. A symmetric type DAC with the diamond culet size of 0.4 mm was used for generating ultra-high pressures,[36] the skeleton drawing of DAC is presented in Fig. 1. The stainless T301 steel gasket was pre-indented to a thickness of 60 μm between two diamond anvils. And a hole of 200 μm in diameter was drilled in the center of the pre-indented area as a sample chamber. A droplet of liquid sample together with a small chip of ruby was loaded into the gasket hole of the DAC. The pressure was measured by the ruby fluorescence.[37]

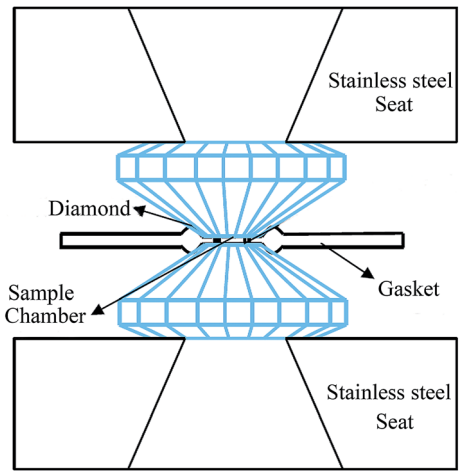

Fig. 1 Schematic illustration of diamond anvil cell. The sample chamber is constructed by two diamond anvils and one drilled stainless steel gasket.

The high-pressure Raman spectra were recorded using an Acton SpctraPro500i spectrograph with a liquid-nitrogen-cooled CCD detector (Princeton Instruments, 1340 × 100) and a 1800 g mm^{-1} holographic grating in a backscattering geometry. The excitation laser was a solid state diode-pumped frequency-doubled Nd:Vanadate laser with a wavelength of 532 nm (Coherent Company). During experiments, the sample image can be projected onto a CCD detector for real-time monitoring. We set the output power as 300 mW, and exposure time of 60 s for all the high-pressure measurements. High-pressure angle dispersive synchrotron XRD experiments were carried out at 13-BM-D station at the Advanced Photon Source (APS), Argonne National Laboratory (ANL). The focused X-ray beam size is 5 × 15 μm^2 for bending magnet device at 13-BM-D, with a wavelength of 0.3344 Å. Fit2D software was used to convert the two-dimensional XRD images into intensity *versus* diffraction angle 2θ patterns.[38]

Results and discussion

The configuration of acetonitrile is charged by the positive methyl and negative nitrile groups and the symmetric point group of the polar acetonitrile molecule is C_{3v} under ambient condition. By factor group analysis, the symmetry of the vibrational modes of acetonitrile can be obtained, disclosing the irreducible representation of acetonitrile as $\Gamma = 5A_1 + A_2 + 6E$. All these 12 modes are Raman active, four of them belonging to symmetry species and the others are double degenerated vibrational modes. Therefore, total eight independent Raman peaks will be observed in the Raman spectrum at ambient condition. Fig. 2 shows the Raman spectrum of acetonitrile at 0, 0.2 and 0.83 GPa, and all independent vibrational modes are denoted on the spectrum.[10,38,39] Besides, three combination modes are also detected: the overtone of the asymmetric C–C≡N bending mode ($2\delta_{CCN}$) locates at 786.01 cm^{-1},[15] the combination of C–C≡N bending and CH_3 methyl rock mode ($\delta_{CCN} + \gamma_{CH_3}$) locates at 1414.7 cm^{-1}, and the combination mode

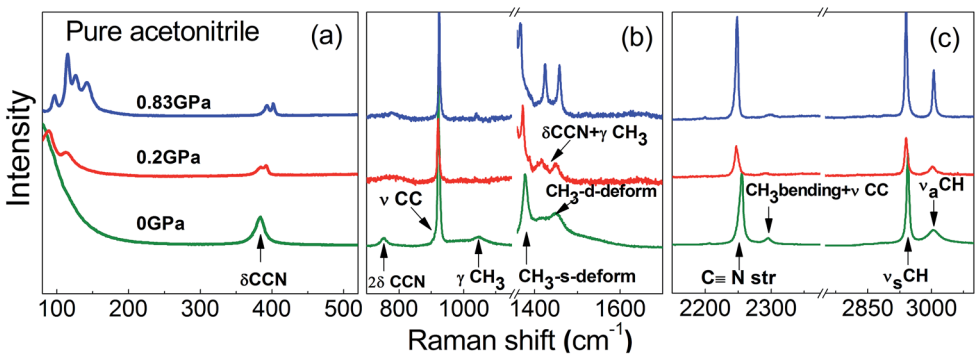

Fig. 2 The Raman spectra of acetonitrile at 0, 0.2 and 0.83 GPa at room temperature. The acetonitrile is liquid at 0 GPa, it turns to α phase at 0.2 GPa and becomes β phase at 0.83 GPa. The Raman vibrational modes are denoted as follows: the asymmetric C–C≡N bending mode (δ_{CCN}), C–C stretching mode (ν_{CC}), CH_3 methyl rock (γ_{CH_3}), CH_3 stretching deformation (CH_3-s-deform), CH_3 degenerate deformation (CH_3-d-deform), the combination band of C–C≡N bending and CH_3 methyl rock mode ($\delta_{CCN} + \gamma_{CH_3}$), the C≡N stretching mode (C≡N str), the combination band of CH_3 bending and C–C stretching mode (CH_3 bending + ν_{CC}), the symmetric C–H stretching mode (ν_sCH) and the asymmetric C–H stretching mode (ν_aCH). The Raman peak of diamond at around 1332 cm^{-1} is removed in the (b).

of CH_3 bending and C–C stretching (CH_3 bending + ν_{CC}) locates at 2292.24 cm^{-1}.[39]

The high-pressure Raman scattering measurements of pure acetonitrile are performed in a diamond anvil cell up to 21.5 GPa at room-temperature. Selected Raman spectra of acetonitrile at different pressures are presented in Fig. 2 and 3a. With pressure increases to 0.2 GPa, the liquid acetonitrile crystallizes into α phase (space group $P2_1/c$), the peak split of the asymmetric C–C≡N bending vibration (δ_{CCN}) is observed and another new peak which derives from the coupling of asymmetric C–C≡N bending mode and asymmetric CH_3 rock appears at around 1414.7 cm^{-1}. When the pressure increases to 0.83 GPa, the transition from α to β phase occurs, where the lattice vibrational modes below 200 cm^{-1} split into 6 individual peaks suddenly, but there are no obvious changes of the internal vibrational peaks crossing this transition. Because the pressure induced fluorescence is enhanced with pressure increasing, the Raman signal of acetonitrile is suppressed and can't be detected clearly when the pressure is higher than 20.18 GPa.

In Fig. 3a, with further increase of pressure, we can see the splitting of the C≡N stretching (2250 cm^{-1}) after 3.87 GPa. For clearly observation, we carry out a curve fitting procedure with Lorentz profile, the fitted spectra is presented in Fig. 4. Although the C≡N stretching peak at 2.21 GPa looks like symmetric, it can be deconvoluted into three Lorentz peaks, this phenomenon is regarded as an overlap of hot band transition,[12,40] but these three peaks split more obviously at high pressures. The pressure dependence of all the Raman vibrations are plotted in Fig. 5, in which we can see that at 4.95 GPa two new peaks appears at 226 cm^{-1} and 415 cm^{-1}, and up to 12.46 GPa, a peak splitting is observed at around 340 cm^{-1} in the lattice vibrational range. Afterwards all the Raman peaks show blue shift upon compression without any splitting.

Previously, a high-pressure Raman study revealed that acetonitrile crystallizes at 0.4 GPa at room temperature and then there is a solid–solid phase transition at 0.6 GPa.[1] It's also pointed by Yenice *et al.*,[3] based on the Raman spectroscopy studies that the freezing pressure of acetonitrile is 0.31 GPa at 296 K, and first solid–solid phase transition from α to β phase locates at 0.57 GPa, moreover, the second solid–solid phase transition from β to γ phase is found at 5.4 GPa. Another Raman investigations from Ma *et al.* indicated that all the three phase transitions, *i.e.* the liquid–α, α–β and β–γ phase transitions occur at 0.4, 0.6 and 9.8 GPa separately.[2] In this study, all three transitions are observed, but the crystallization pressure is found to be 0.2 GPa, much lower than that given by previous studies. The α–β phase transition is around 0.83 GPa, while for the β–γ phase transitions is suggested to start from 4.95 GPa

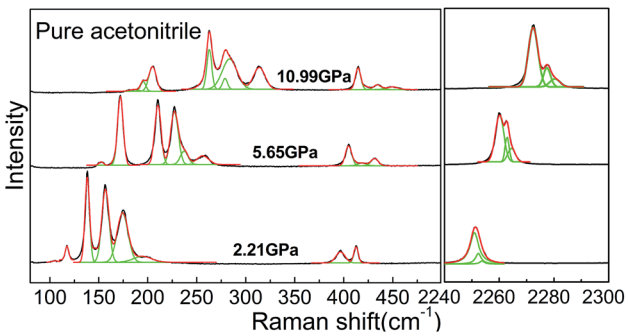

Fig. 4 Raman spectra of pure acetonitrile (low frequency and C≡N stretching mode at 2250 cm^{-1}) at different pressures, multiple peaks fitting with Lorentz profile curves are shown as green lines.

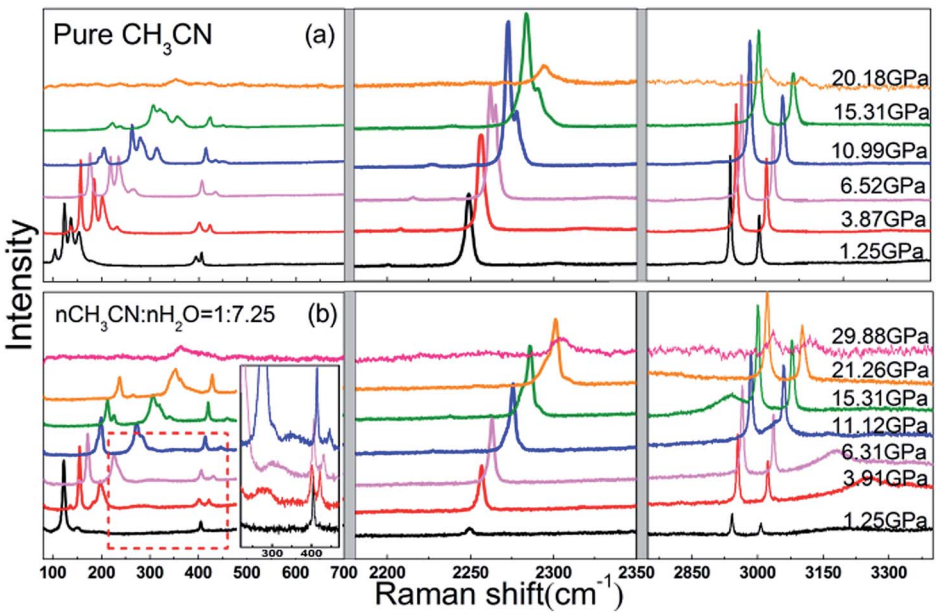

Fig. 3 The Raman spectra of pure acetonitrile (a) and acetonitrile–water mixtures (b) in the similar pressure region from 1.25 to 21.26 GPa at room temperature.

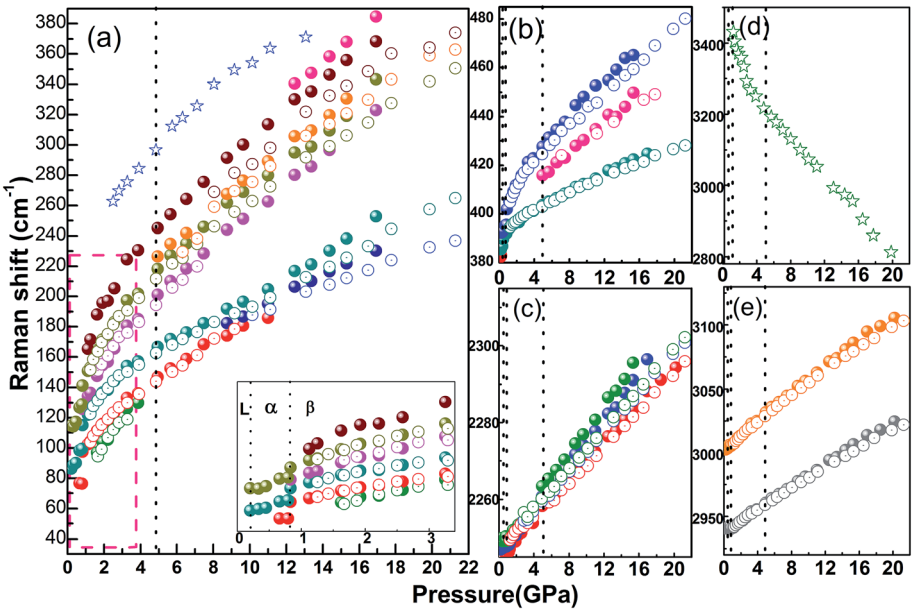

Fig. 5 Pressure dependence of Raman shifts of acetonitrile (solid symbols) and acetonitrile–water mixtures (empty symbols) at room temperature, the Raman spectrum in the low wavenumber region (a) is amplified. The vertical dashed lines are functional guide for the phase transition pressures in pure acetonitrile, and a peak splitting is observed at around 340 cm^{-1}. The translational vibration and the O–H stretching of ice–VII clusters are shown by empty star symbols.

based on the emergence of two new peaks, at the same time, we pay additional attention to the C≡N stretching. As this was deconvoluted into three individual peaks, the differences between these peak positions are plotted and shown in Fig. 6. If the three peaks are marked as no. 1 to 3 from low to high wavenumber side, the peak position differences between the first and second peaks (no. 2-1), as well as between the first and third peaks (no. 3-1) is calculated. Obviously, these peak to peak values decrease firstly and start to ascend after 4 GPa. Being consistent with the emergence of the new peaks, the transition from β to γ phase is suggested to occur within a pressure range from 4.95 to 12.46 GPa, between this range the two phases coexist.

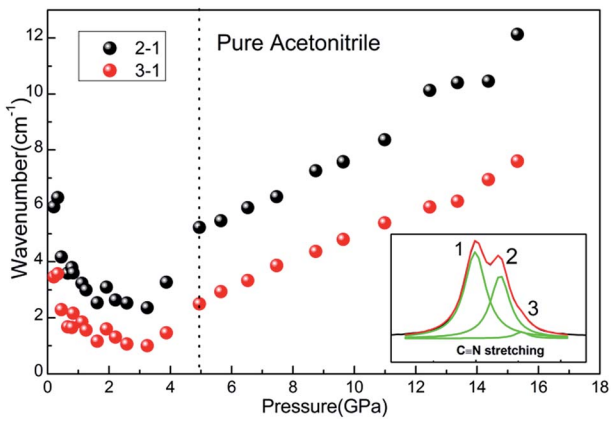

Fig. 6 Pressure evolution of the peak to peak values for deconvoluted C≡N stretching, the signed peak number is indicated in the insert spectrum.

In addition, with further increasing pressure, the intensity of Raman peaks decreases gradually, while the background in spectra grows dramatically. This is probably due to the pressure-induced some kind of polymerization so that the fluorescence appears and grows with pressure. In order to confirm that such high background comes from growing fluorescence, we checked the Raman signal using 647 nm laser as excitation, then photoluminescence is observed with the low energy laser. Then we measured the Raman spectra of the unloading sample through two polarizers, the result indicates that appearance of the Raman peak has no direct relationship with the polarization. Moreover, we also checked the infrared spectrum of condensed acetonitrile. Therefore, we think that such high background comes from growing fluorescence in Raman spectrum. It is suggested that the acetonitrile ultimately transforms into an amorphous state,[2] as the pressure may induces an irreversible breaking of the C≡N bond. Under high pressures, the distances between molecules or atoms are decreased, so that the interaction or bond type among the system may be changed, especially in molecular crystal systems.[41,42] Similarly, chemical reaction may occur through bond reconstruction or reformation, resulting in polymerization which often occurs in supermolecule.[43,44] Here we found that the acetonitrile does not turn to initial liquid state after it is condensed to highest pressure and then released to 0 GPa. Meanwhile the pressure induced fluorescence is reserved to ambient condition indicating that irreversible chemical reaction or polymerization occurs, this is also convinced that no Raman signal is detected for the recovered sample.

The Raman spectra of the acetonitrile–water mixture are presented in Fig. 3b, to reflect the relevant changes and phase

transitions of two samples intuitively. Obviously, the main vibrations of acetonitrile can be found in the mixture sample, but all of their peak intensities are weaker than the pure acetonitrile, and the relative distribution of peak intensity shows little difference. For clear comparison, the Raman shifts of pure acetonitrile and acetonitrile–water mixtures as a function of pressure are shown in Fig. 5. As the acetonitrile–water aqueous solution is very complex system, its structure may change depending on the concentration distribution. The molar ration of $n\mathrm{CH_3CN}$: $n\mathrm{H_2O}$ we used here is 1 : 7.25, *i.e.* X_{AN} equals to 0.12, and this value falls in the range of $X_{\mathrm{AN}} \leq 0.2$, where small acetonitrile clusters would be isolated from extended water hydrogen bond network at ambient condition. When compressed under pressure, there are probable fluctuations of density and concentration, or phase separation may occur at solidification point.

In the acetonitrile–water mixture, characteristic Raman peaks of acetonitrile are found, and the transition from β to γ phase is detected, suggesting the crystallization of acetonitrile clusters in the mixture. In the same way, we observed the translational vibration (around 270 $\mathrm{cm^{-1}}$ at 3 GPa) and the O–H stretching (around 3250 $\mathrm{cm^{-1}}$ at 3 GPa) which belongs to ice–VII.[45,46] These vibrations of pure ice–VII under high pressure were also measured for double check confirming the existence of ice–VII clusters in the mixture. The pressure dependence of these two peaks is denoted by star symbols in Fig. 5a and d, respectively. The broad translational vibration has weak intensity, the enlarged view of selected spectra are presented in Fig. 3b. On the other hand, two vibrations form ice–VII are observed and the O–H stretching gives a negative slope against pressure. This is due to the elongation of the covalent O–H bond as the bond length of O–H···O–H hydrogen-bonds, as well as the heterogeneous O–H···N≡C hydrogen-bonds decreases under high pressure.

Now we can take a look at what happens in the acetonitrile–water mixture. Since water is the main content, the acetonitrile is supposed to be surrounded by water which forms a hydrogen bond network in the mixture, which was convinced in the liquid state.[12,15,30] With increasing pressure, the mixture remains liquid up to 1.25 GPa where it solidifies suddenly, therefore α phase of acetonitrile is skipped, the measured Raman spectra shows characteristic peaks similar to β acetonitrile. Comparing with pure acetonitrile, the splitting of C–C≡N bending vibration (δ_{CCN}) and variation of C≡N stretching mode are also detected in the mixture, *i.e.* the characteristic signal indicates the transition from β to γ phase, but the transition pressure is postponed to about 7 GPa. It also can be seen that the vibration frequency is depressed in the mixture sample, the frequency difference between acetonitrile and acetonitrile–water mixture becomes larger with pressure goes higher. On the other hand, at similar pressure, the vibrational differences between pure acetonitrile and the mixture for different vibration modes are diverse. More specifically, the intramolecular vibrations at low frequencies show a large difference as shown in Fig. 5a, while the high frequency vibrations of C–H stretching mode locate at around 3000 $\mathrm{cm^{-1}}$ gives a relatively small difference (Fig. 5e), finally the C≡N stretching at around 2250 $\mathrm{cm^{-1}}$ show a minimum difference due to the strong interaction of C≡N bond (Fig. 5c). Moreover, the peak intensity of C≡N stretching mode for pure acetonitrile and the mixture presents a different behavior which reflects the influence of different surrounding.[15,40]

It is suggested that both acetonitrile and water domains coexist in the mixtures and interact with each other through hydrogen bonds in the solid state, like the similar effect in the liquid state. According to the XRD study, Takamuku *et al.*[15] revealed that the acetonitrile–acetonitrile interactions would be strengthened in water solutions, and the small acetonitrile clusters would form in the mixtures and dipole–dipole interaction between acetonitrile and water molecules become weak then. But with the decrease of acetonitrile content, the acetonitrile clusters would be disrupted when the X_{AN} of the mixtures becomes lower than 0.2.[10,47] This means more single acetonitrile molecules exists and is surrounded by water molecules at $X_{\mathrm{AN}} <$ 0.2. When pressure is increased and the solidification point is approaching, there may be some fluctuations of density or concentration and final aggregation of same molecules to clusters.

Comparing with pure acetonitrile and the acetonitrile–water mixture, the splitting of C–C≡N bending vibration (δ_{CCN}) and variation of C≡N stretching modes detected in the mixture starts at a relatively higher pressure. The C–C≡N bending vibration (δ_{CCN}) split is observed above 7 GPa, it suggests the acetonitrile solidifies into clusters mixtures and the solidified ice crystals surrounds these acetonitrile clusters, forming small domains of acetonitrile and ice crystals, and the acetonitrile crystals in β phase is extended to above 7 GPa much higher than that in pure acetonitrile. Another noteworthy point is that the fluorescence is depressed in the mixture sample. For pure acetonitrile, the fluorescence background is enhanced with pressure increasing, and no Raman peaks can be detected above 20.18 GPa. For the mixed sample, the Raman peaks can be detected even after being treated up to 29.88 GPa, so it is supported that surrounded ice domains around acetonitrile clusters provides a relative soft environment. Upon decompression, the Raman signal of acetonitrile–water mixture doesn't recover and the fluorescence remains, like the pure acetonitrile.

In order to check the crystal structures of acetonitrile–water mixture under high pressure, synchrotron XRD measurements were performed at room temperature. Fig. 7 shows synchrotron XRD patterns of acetonitrile–water mixtures collected at 7.44 GPa. The diffraction pattern is indexed with DICVOL91 method using Material Studio software. The diffraction peaks of β acetonitrile in orthorhombic system with space group $Cmc2_1$ and ice VII in cubic system with space group of $Pn\bar{3}m$ are denoted by red and blue bars as shown in Fig. 5.[48–50] Besides these peaks, several unknown peaks are marked by black asterisks in the pattern, which comes from unknown structure of the acetonitrile–water mixture crystallization. As the crystal structure of γ acetonitrile has been studied by high pressure neutron scattering measurements,[51] we also compared our unknown structure with the γ phase and confirmed that it's different with γ acetonitrile. Unfortunately, this unknown structure in acetonitrile–water mixture is hard to resolve with only ten peaks, so we index the

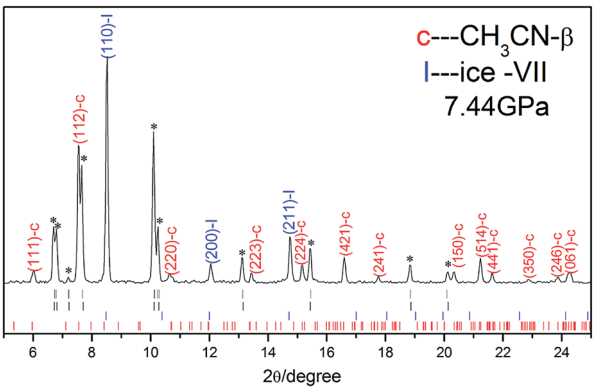

Fig. 7 High-pressure XRD patterns of acetonitrile–water mixtures at room temperature. The newly emerging peaks are marked by asterisk. The upper gray tick marks represent the indexing peak positions for the structure I, and the lower represent structure II. The other two is for the ice–VII and CH_3CN-β, respectively.

unknown peaks with DICVOL91 Power Indexing and found two possible structures, one of which is an orthorhombic structure (I), with the lattice parameters of $a = 7.49(7)$ Å, $b = 6.58(9)$ Å, $c = 5.67(6)$ Å, and $V = 280.43$ Å^3, and another is the monoclinic structure (II), with the lattice parameters of $a = 5.76(1)$ Å, $b = 5.10(4)$ Å, $c = 3.41(5)$ Å, and $V = 99.42$ Å^3. To find detailed structure further experimental studies are needed.

Conclusions

In conclusion, the structural behaviours of pure acetonitrile and acetonitrile–water mixture with molar ratio of 1 : 7.25 were investigated by Raman scattering at room temperature. It is suggested that pure acetonitrile transformed from liquid to α phase, then to β phase and finally into γ phase at 0.2 GPa, 0.8 GPa and 4.95 GPa, respectively. While in acetonitrile–water mixture the much higher solidification pressure is found up to 1.25 GPa and the sustained β phase remains until 7 GPa. Moreover, the fluorescence is depressed in the mixture sample. For pure acetonitrile, no Raman peaks can be detected above 20.18 GPa. But for the mixed sample, the Raman peaks can be detected even after being treated up to 29.88 GPa. After pressure is released, both of the Raman signals of two samples don't recover and the fluorescence remains. In acetonitrile–water mixture, small clusters of acetonitrile are supposed to exist as separated domains and be surrounded by hydrogen bond network of ice crystals. Two possible structures of the acetonitrile–water mixture are proposed by indexing the unknown peaks observed in the X-ray diffraction pattern collected at 7.44 GPa. The study of acetonitrile–water mixtures under high pressure provides significant information for better understanding of the physical properties of acetonitrile aqueous solution under extreme conditions.

Acknowledgements

This work was financial supported by the National Basic Research Program of China (No. 2011CB808200), the National Natural Science Foundation of China (No. 91014004, 11274137, 11074090, 11004074, 11474127), Specialized Research Fund for the Doctoral Proensgram of Higher Education (Grant No. 20100061120093) and National Found for Fostering Talents of Basic Science (No. J1103202). The XRD experiments of this work were performed at GeoSoilEnviroCARS (Sector 13), Advanced Photon Source (APS), Argonne National Laboratory. GeoSoilEnviroCARS is supported by the National Science Foundation – Earth Sciences (EAR-1128799) and Department of Energy – GeoSciences (DE-FG02-94ER14466). This research used resources of the Advanced Photon Source, a U.S. Department of Energy (DOE) Office of Science User Facility operated for the DOE Office of Science by Argonne National Laboratory under Contract No. DE-AC02-06CH11357.

References

1 H. Yamawaki, K. Aoki, Y. Kakudate, M. Yoshida, S. Usuba and S. Fujiwara, *Chem. Phys. Lett.*, 1990, **169**, 77–80.
2 C. Ma, F. Huang, X. Wu, H. Cui, F. Li, H. Zhu, Q. Zhou and Q. Cui, *RSC Adv.*, 2013, **3**, 1509–1513.
3 K. M. Yenice, S. A. Lee and A. Anderson, *J. Raman Spectrosc.*, 1996, **27**, 835–840.
4 A. Olejniczak and A. KatrusiakAnna, *J. Phys. Chem. B*, 2008, **112**, 7183–7190.
5 T. Brackemeyer, G. Erker, R. Fröhlich, J. Prigge and U. Peuchert, *Chem. Ber.*, 1997, **130**, 899–902.
6 R. Enjalbert and J. Galy, *Acta Crystallogr., Sect. B: Struct. Sci.*, 2002, **58**, 1005–1010.
7 M. Jabbari, *J. Mol. Liq.*, 2015, **208**, 5–10.
8 D. Sazou, *Synth. Met.*, 2002, **130**, 45–54.
9 T. Takamuku, Y. Noguchi, M. Matsugami, H. Iwase, T. Otomod and M. Nagaoe, *J. Mol. Liq.*, 2007, **136**, 147–155.
10 M. Tabata, M. Kumamoto and J. Nishimoto, *Anal. Chem.*, 1996, **68**, 758–762.
11 C. Oldiges, K. Wittler, T. Tönsing and A. Alijah, *J. Phys. Chem. A*, 2002, **106**, 7147–7154.
12 D. Jamroz, J. Stangret and J. Lindgren, *J. Am. Chem. Soc.*, 1993, **115**, 6165–6168.
13 J. E. Bertie and Z. Lan, *J. Phys. Chem. B*, 1997, **101**, 4111–4119.
14 M. Stoev, A. Makarow and J. M. A. Robledo, *Spectrosc. Lett.*, 1995, **28**, 1251–1258.
15 T. Takamuku, M. Tabata, A. Yamaguchi, J. Nishimoto, M. Kumamoto, H. Wakita and T. Yamaguchi, *J. Phys. Chem. B*, 1998, **102**, 8880–8888.
16 K. Nishikawa, Y. Kasahara and T. Ichioka, *J. Phys. Chem. B*, 2002, **106**, 693–700.
17 R. E. Robertson and S. E. Sugamori, *J. Am. Chem. Soc.*, 2002, **91**, 7254–7259.
18 Y. Marcus and Y. Migron, *J. Phys. Chem.*, 1991, **95**, 400–406.
19 M. Nakamura, K. Tamura and S. Murakami, *Thermochim. Acta*, 1995, **253**, 127–136.
20 A. J. Easteal and L. A. Woolf, *J. Chem. Thermodyn.*, 1988, **20**, 701–706.
21 M. Sakurai, *J. Chem. Eng. Data*, 1992, **37**, 358–362.

22 F. H. Tukhvatullin, A. Jumabaev, G. Muradov, H. A. Hushvaktov and A. A. Absanov, *J. Raman Spectrosc.*, 2005, **36**, 932–937.
23 G. V. Kabisch, *Z. Phys. Chem.*, 1982, **263**, 48–60.
24 K. L. Rowlen, J. M. Harris and A. Chem, *Anal. Chem.*, 1991, **63**, 964–969.
25 Y. Marcus, *J. Phys. Org. Chem.*, 2012, **25**, 1072–1085.
26 J. Chen and P. H. L. Sit, *Chem. Phys.*, 2015, **457**, 87–97.
27 H. Kovacs and A. Laaksonen, *J. Chem. Soc.*, 1991, **113**, 5596–5605.
28 E. V. Goldammer and H. G. Hertz, *J. Phys. Chem.*, 1970, **74**, 3737–3755.
29 A. J. Easteal, *Aust. J. Chem.*, 1979, **32**, 1379–1384.
30 H. Leiter, K. J. Patil and H. G. Hertz, *J. Solution Chem.*, 1983, **12**, 503–517.
31 J. E. Bertie and Z. Lan, *J. Phys. Chem. B*, 1997, **101**, 4111–4119.
32 J. R. Reimers and L. E. Hall, *J. Chem. Soc.*, 1999, **121**, 3730–3744.
33 M. Hurth and D. Woermann, *Berichte der Bunsengesellschaft für Physikalische Chemie*, 1987, **91**, 614–616.
34 D. Pfenning and D. Woermann, *J. Membr. Sci.*, 1987, **32**, 105–116.
35 K. Nishikawa, Y. Kasahara and T. Ichioka, *J. Phys. Chem. B*, 2002, **106**, 693–700.
36 W. Paszkowicz, *Nucl. Instrum. Methods Phys. Res., Sect. B*, 2002, **198**, 142–182.
37 H. Mao, J. Xu and P. Bell, *J. Geophys. Res.*, 1986, **91**, 4673–4676.
38 A. Hammersley, S. Svensson, M. Hanfland, A. Fitch and D. Hausermann, *High Pressure Res.*, 1996, **14**, 235–248.
39 E. Pace and L. J. Noe, *J. Chem. Phys.*, 1968, **49**, 5317–5325.
40 A. Loewenschuss and N. Yellin, *Spectrochim. Acta, Part A*, 1975, **31**, 207–212.
41 C. S. Yoo, *Phys. Chem. Chem. Phys.*, 2013, **15**, 7949–7966.
42 F. Datchi, S. Ninet, M. Gauthier, A. M. Saitta, B. Canny and F. Decremp, *Phys. Rev. B: Condens. Matter Mater. Phys.*, 2006, **73**, 174111.
43 M. Santoro, L. Ciabini, R. Bini and V. Schettino, *J. Raman Spectrosc.*, 2003, **34**, 557–566.
44 K. Aoki, S. Usuba, M. Yoshida, Y. Kakudate, K. Tanaka and S. Fujiwara, *J. Chem. Phys.*, 1988, **89**, 529–534.
45 G. Walrafen, *J. Chem. Phys.*, 1964, **40**, 3249–3256.
46 G. Walrafen, *J. Chem. Phys.*, 1967, **47**, 114–126.
47 M. Ueno, S. Ueyama, S. Hashimoto, N. Tsuchihashi and K. Ibuki, *J. Solution Chem.*, 2004, **33**, 827–846.
48 G. E. Walrafen, M. Abebe, F. A. Mauer, S. Block, G. J. Piermarini and R. Munro, *J. Chem. Phys.*, 1982, **77**, 2166–2174.
49 B. Kamb, *Science*, 1965, **150**, 205–209.
50 M. Somayazulu, J. Shu, C.-S. Zha, A. F. Goncharov, O. Tschauner, H.-K. Mao and R. J. Hemley, *J. Chem. Phys.*, 2008, **128**, 064510.
51 H. Zheng, K. Li, G. Cody, C. Tulk, J. Molaison, W. Yang, I. Ivanov, M. Guthrie and H. K. Mao, *Congress and General Assembly of the International Union of Crystallography*, Abstract, 2014, MS49, P08.

